

AUTOMATION OF FOCUSING SYSTEM BASED ON IMAGE PROCESSING THROUGH INTELLIGENT ALGORITHM

¹MAHMOUD A. ELESAWY, ²MOSTAFA R.A. ATIA, ³MOHAMED I. ABU EL-SEBAH

^{1,2}Mechanical Engineering Department ARAB ACADEMY FOR SCIENCE, TECHNOLOGY AND MARITIME
TRANSPORT Egypt

³ELECTRONIC RESEARCH INSTITUTE Egypt

E-mail: ¹essawy@aast.edu, ²mrostom1@aast.edu, ³mohamedibrahim32@hotmail.com

Abstract— There are a number of precise measurement and inspection applications, which are based on image processing. Focusing is a major step to accomplish these applications, especially when microscopic images are required. Microscopic manual focusing based on expert's eye could result in misleading decisions since it is subjected to human accuracy, sensitivity and visual capabilities. Therefore, automatic focusing systems have been developed to increase accuracy with better reliability and save time. In this research, an auto focusing mechanical module with integrated software is designed, tested and verified. This system is based on grasping a sequence of images using coarse and fine focusing mechanisms. The most focused image is identified through an algorithm, which encapsulates various focusing approaches. These approaches are Image Curvature (CURV), Tenengrad based algorithms (TENG), Squared Gradient (GRAS) and Gray Level Variance (GLV). The aim of this research is making a comparison between these approaches to select the best when used with microscopic images of un-etched gray cast iron specimens. The proposed auto focusing module is a step towards the automation of manual focusing systems in microscopes.

Keywords— Microscope, Auto Focusing, Manual Focusing, Algorithm, Focal Value, Focusing Approaches, Mechanical Module.

I. INTRODUCTION

For any image to be put into focus with clear details, it must be put into an appropriate distance with the lens required to capture the image. Out of focus images can't be put into focus by mean of image processing techniques since there are missing data that can't be retrieved. Manual focusing has become a tiring and intangible task. Thus, the need of automatic focusing has arisen as a challenging and demanding need in several applications. Auto focusing is essential for analyzing the details of solid samples with complex surfaces, auto focusing systems usually focus much better and more consistently than manual focusing and this is important for researchers to get high quality images especially for image processing applications[1]. Moreover, Auto focusing (AF) is an important technique that is needed in many applications that requires precise measurement and inspection. This technique is currently developed more focusing on high speed implementation and under a microscopic view[2]. The aim of metallurgical investigation is to obtain data regarding the internal microstructure of any material. Thus, affects the study of fracture surfaces, crack formation, corrosive attack, and deformation phenomena on the surface. Auto focusing is a powerful topic in literature and lots of focusing algorithms have been proposed, the choice of an appropriate focusing technique for certain experimental work remains time consuming and challenging [3]. Auto focusing is highly responsible for replacing the function of the expert's eye and reducing the percentage of error while focusing. Therefore implementation of AF in software is much desired in industrial applications[2].

Different previous literatures has adopted the automation of the focusing system in microscopes like in [4] , [1], [5] using different focusing techniques as illustrated through this paper in section 3. Moreover, others have used focusing techniques on different images for a various range of applications like in [6], [7], [8]. In this paper, an auto focusing mechanical module with integrated software is designed, tested and verified. This module can be attached to a coaxial fine/coarse focus system in the microscope in order to automate the focusing process. Since distance between lens and object determines the sharpness of an acquired image, that indicates the focus degree of the image, this degree of focus is quantified as a Focal Value (FV) Then, a FV curve forms as the lens position and acquired image vary. Such a curve might show a peak where the acquired image contents have the sharpest details[2]. AF task is to search for a focused position via comparing the FVs of the acquired images. Methods for FV measurement were developed based on the image histogram, variation, energy of squared gradient, entropy function, frequency spectrum function, energy of Laplacian, square Gaussian gradient, Laplacian, Gaussian and Tenengrad based algorithms. Most of the measures perform good efficiency on computation. This might induce a significant local peak in an FV curve and result in inaccurate results and decisions[2]. Through the extensive survey illustrated in the previous table, several properties of different algorithms were concluded. Gray level variance (GLV) measures the variations in gray levels among the image pixels where bright and dark pixels have the same effect.

Table 1: Cross Mapping of Researches and Chosen Techniques

	1	2	3	4	5	6	7	8	9	10	11
[1]							✓				
[2]	✓					✓	✓				
[3]	✓			✓							
[5]			✓				✓				
[6]	✓										
[8]				✓			✓				
[9]	✓	✓									
[10]				✓	✓		✓				
[11]	✓	✓			✓						
[12]										✓	
[13]	✓				✓		✓				✓
[14]				✓							
[15]		✓									
[16]	✓			✓					✓	✓	✓
[17]	✓	✓		✓							
[18]							✓	✓			
[19]	✓										
[20]	✓						✓				

The techniques stated in literature are as follows; 1) GLVA – 2) CURV – 3) GDER – 4) GRAS – 5) HISE – 6) SFRQ – 7) TENG – 8) VOLA – 9) SFIL – 10) DCT – 11) ACMO

Such algorithm is a very straightforward technique for traditional microscopes. Vollath's measure (VOLA) and Histogram entropy (HISE) both compromised good focusing results with low information content images. Tenengrad based algorithms (TENG) and Squared Gradient (GRAS) performed well during the existence of false maxima near the absolute maximum. Moreover, Gaussian derivative (GDER) respond to the best focus position with a local maximum consuming long processing time. Spatial frequency (SFRQ) and Steerable filters (SFIL) based algorithms has shown good results in detecting image edge sharpness and are widely used in image fusion and measuring image clearness and texture. SFIL is also used in image enhancement and feature extraction. Discrete cosine transform (DCT) represented the image in spatial frequency domain showing details of very low and very high frequencies that were difficult to measure in time domain. Absolute central moment (ACMO) measures statistically the variability of the gray levels of an image with respect to the local mean.

This research paper is organized as follows: Section 2 discusses the mechanical hardware system proposed. Section 3 discusses several auto focusing algorithms previously used and the criteria upon which only four of them were chosen. Section 4 discusses the details of the proposed system integrating the hardware

system with the suggested algorithm used to autofocus on an image. Section 5 illustrates a case study that shows the steps in details of capturing an in focus image automatically through the proposed system.

II. THE MECHANICAL SYSTEM PROPOSED

The main objective behind proposing this mechanical module is to automate the focusing of a microscope that already involves manual focusing approaches. Therefore, a microscope with coaxial coarse/fine focusing system was chosen to be part of the design. The specifications of the chosen microscope will be illustrated in details with the components of the proposed mechanical system.

2.1. The Microscope Used: Innovatest IN-MM600

The chosen microscope for the task, shown in **Error! Reference source not found.**, is an inverted microscope of model Innovatest IN- MM600. A CCD camera is attached directly to the microscopic setup, and is connected to the host computer through a 10moons video capture card. The microscope consists mainly of a stage and a stage plate, coaxial coarse and fine focusing knob and an objective stage holding the 4 rotating lens with different magnifications.

2.2. The Mechanical Module

The proposed mechanical module is supposed to be attached to the focusing knobs as shown in **Error! Reference source not found.** This module consists of 4 pulleys each located at a specified place. One is attached to the coarse knob of the microscope while another is attached to a stepper motor expected to drive the coarse knob. Those two pulleys are enrolled together through a belt and are tightly distanced to ensure efficient performance. Similar pulley belt arrangement is designed for the fine knob. This mechanical module is used for motion transmission between the actuators and the rotating knobs responsible for focusing.

III. IMAGE FOCUSING TECHNIQUES

Focusing techniques is the key in auto focusing systems. The focus function must calculate a certain values and indicates the quality of a series images[1]. Several algorithms through previous literature were found to measure the FV of an image. Each of these algorithms measures a specific and different feature of the image that identifies the degree of focus. The output of an ideal focusing technique is defined as having a maximum value at the best focused image and decreasing as a defocus increases[3]. By surveying a number of algorithms commonly used in previous research, it was found that there are specific algorithms that have shown accurate and precise results of most focused images over the other used techniques. Despite most of focusing algorithms almost give same decision of the most focused

captured microscopic image; each single algorithm depends on different relations between image pixels. Typical methods for measuring the image FV are used. In this paper, various techniques were involved in the computer experimentation. In the upcoming section, the most commonly used focusing techniques are illustrated and described individually in details.



Fig.1. Real scene of the Mechanical system

3.1. Gray Level Variance (GLV)

A well-focused image is expected to have a high variation in gray levels, the local variance at point (m, n) , with $m=1...M$ and $n=1...N$ is given by[12] :

$$VAR(I) = \frac{1}{NM} \sum_m^M \sum_n^N ([I_v(m, n) - \bar{I}_v]^2) \quad (1)$$

The focus measure based on the local variance will be given by the global variance.

Where $N*M$ the window size at centre point (m, n) and \bar{I}_v is the mean level gray value given by:

$$\bar{I}_v = \frac{1}{NM} \sum_m^M \sum_n^N I_v(m, n) \quad (2)$$

3.2. Threshold and Squared Gradient (GRAS)

Sharpness implies the high frequency components of an image so high pass filters are often used to extract high frequency portions of an image[21]. This algorithm sums squared differences of derivatives of pixels gray levels, making larger gradients exerts more influence[3]. The focal value can be calculated as follows:

$$F_{sq_grad} = \sum_{Height} \sum_{Width} (i(x+1, y) - i(x, y))^2 \quad (3)$$

Such that $(i(x+1, y) - i(x, y))^2 \geq \theta$ and θ is a threshold value.

Vertical Squared Gradient:

$$F_{sq_grad_Ver} = \sum_{x=0}^{M-1} \sum_{y=0}^{N-2} (f(x+2, y) - f(x, y))^2 \quad (4)$$

Horizontal Squared Gradient:

$$F_{sq_grad_Hor} = \sum_{x=0}^{M-2} \sum_{y=0}^{N-1} (f(x, y+1) - f(x, y))^2 \quad (5)$$

3.3. Image Curvature (CURV)

Sharper image region implies a higher gray value variance. Therefore if the gray level values are treated as a 3D surface $(x, y, g(x, y))$, the curvature in a

sharp image region is expected to be higher than in an unsharp region[9]. If the image gray levels are interpolated by means of a surface, the curvature of this surface may be used as a focus measure. The first step of calculating this focus measure is to approximate the surface $f(x, y) = P_0X + P_1Y + P_2X^2 + P_3Y^2$, the vector coefficients $P = (P_0, P_1, P_2, P_3)^t$ is computed through least square approximation by applying 2 convolution masks g_0 and g_2 .

$$g_0 = \begin{pmatrix} -1 & 0 & 1 \\ -1 & 0 & 1 \\ -1 & 0 & 1 \end{pmatrix} \quad g_2 = \begin{pmatrix} 1 & 0 & 1 \\ 1 & 0 & 1 \\ 1 & 0 & 1 \end{pmatrix} \quad (6)$$

$$P = \left(\frac{g_0 * g}{\sigma}, \frac{g_0^t * g}{\sigma}, \frac{3g_2 * g}{10}, \frac{g_2^t * g}{\sigma}, -\frac{g_2 * g}{\sigma} + \frac{3g_2^t * g}{10} \right)^t \quad (7)$$

At each pixel, the gray level intensity is calculated and then calculating the coefficients of the surface. The next step is to combine these coefficients in order to obtain a sufficient focus measure[9].

3.4. Tenengrad based algorithms (TEN)

The Tenengrad focus measure, measures the sum of the squared responses of a horizontal and a vertical Sobel mask.

This calculation is derived from Sobel operator:

$$C_{TEN} = \sum_{x=2}^{M-1} \sum_{y=2}^{N-1} [\nabla S(x, y)]^2 \quad \text{For } \nabla S(x, y) > T \quad (8)$$

Where T is a selected threshold value and $\nabla S(x, y)$ is a Sobel gradient expressed as:

$$\nabla S(x, y) = \sqrt{\nabla S_x^2(x, y) + \nabla S_y^2(x, y)} \quad (9)$$

This measure convolves the image with vertical (S_x) and horizontal (S_y) Sobel operators. To get a global measure over the whole image, the square of the gradient vector components are summed[22].

$$F_{Tenengrad} = \sum \sum S_x(x, y)^2 + S_y(x, y)^2 \quad (10)$$

IV. THE PROPOSED FOCUSING SYSTEM

The proposed system consists mainly of a combination between hardware components previously discussed and software based algorithm. The components of the hardware contain a metallurgical inverted microscope, computer, CCD camera connected to the microscope, data acquisition interfacing and the mechanical test rig illustrated earlier in section 2. The mechanical test rig is attached to the microscope through its focusing knobs. The focusing knobs are coaxial coarse/fine wheels responsible for positioning the objective lens which defines the degree of focus of the test specimen in the current scene (position). The flow chart in **Error! Reference source not found.**

illustrates the operation of the whole system in details. At first, the coarse knob is

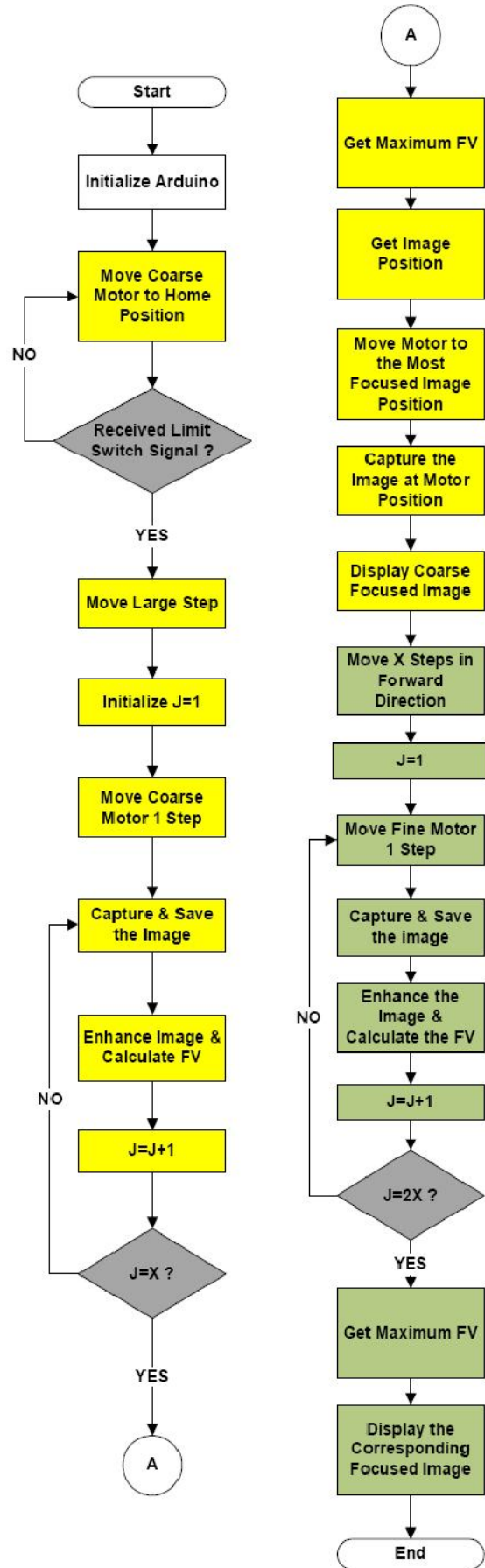


Fig.2. The flow chart of the proposed system

forced to return back to its home position using a mechanical switch. Starting from the home position, the coarse knob rotates in the forward direction with larger steps so as to overcome the dead-band range of focus that surely doesn't contain the most focused image. These large steps are variable according to the magnification of the objective lens. After passing the dead-band region, a set of images is captured at specific steps. Each step of the stepper motor is transmitted as one degree of rotation in the pulleys of the mechanical system. After capturing, the images were saved individually with their corresponding positions. The saved images are then enhanced and the Focal Value (FV) of each image is then calculated according to the chosen algorithm discussed. The image with maximum FV is then determined to be the most focused image and its corresponding position is then identified. Next step involves returning the coarse knob back to the pre-identified most focused image position. This way the coarse knob has finished its job and it's time for refining the focus using the fine knob. The fine knob starts rotating in the forward direction with a specific number of steps and then stops to start image capture. A set of images is then captured and saved through a wider range in the backward direction. The captured images are then enhanced and the FVs are calculated. The maximum FV is also determined and its corresponding image position. The image with the maximum FV (by fine knob) is then displayed.

V. CASE STUDY

In order to test the behavior of the focusing techniques, a focusing curve is drawn for each technique that defines the variation of FV between captured images at different positions. Curves are obtained similarly for both knobs i.e coarse and fine knobs. The samples used in this experiment are metallurgical samples of cast iron. Fig.1. Samples in silica gel shows a number of the tested samples prepared for microscopic examination. In this experiment, 11 different cast iron samples were investigated, 4 different positions were examined in each sample and 11 focusing techniques were tested on all of the samples using all of the positions. The used samples are shown in Fig.1.

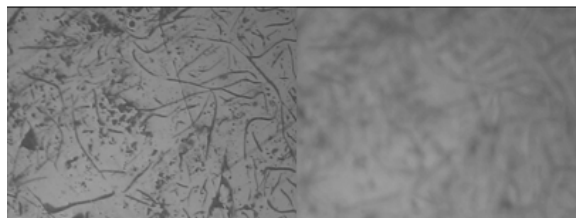


Fig.1. Samples in silica gel

Two sample images at two different lens positions are shown in Focused Blurred

Fig.2.

The left image is observed to be visually in focused while the right image is blurred i.e out of focus.



Focused Blurred

Fig.2. Focused and Blurred images

5.1. Experimental Test

In this research, four selected focusing techniques were tested and examined on various microscopic metallurgical samples. The results indicating the performance of these four techniques are shown below. Focal value of the sample was calculated using CURV, GLV, TENG and GRAS. For each technique, the proposed algorithms were run targeting to locate the most focused image in the tested sample.

5.2. Coarse Knob Results

The generated curve shown in Fig.3 demonstrates the focal values of the set of captured images using the coarse knob of the microscope. Curves of the four different focal value measuring techniques are overlapped together to show variation in measuring criteria. Even though the four algorithms have successfully agreed to allocate the most focused image of the set of 24 images to be image number 17, there's still a remarkable difference in the curve trend of each algorithm separately. For comparison purposes, calculated FVs are normalized to help compare between the algorithms separately. In TENG curve, it's observed that there are many steep fluctuations in FV from 0.03 till 0.1 that appears in the early stage of out of focus images until a sudden peak is observed in image 17, that's the most focused one. Gradual decrease in the focal value is yet again observed with the same fluctuating trend as we go far from the focused image again i.e the objective gets closer to the sample. In GLV, it's observed that the FV starts with a high value of around 0.85 and then the FV decreases gradually over a wide range of images ranging from 1 till image 16, then a sudden peak is observed at image 17. The curve then decreases sharply over a narrow range of images ranging from image 18 till 24. In both CURV and GRAS, the FV fluctuates above the zero but below 0.1 over a wide range of images ranging from image 1 till image 16, then a sharp peak in FV appears with a maximum FV of 0.98 at image 17. In the remaining out of focus images range from image 18 till 24, a remarkable deterioration in the FVs is observed to

bound again the FVs below 0.1. It's concluded that TENG, GRAS and CURV all can determine the most focused image in a range of images in a significant way where there's a remarkable difference between the most focused image and the out of focus ones. However, GLV has shown same results for the most focused image but the unexpected increase and decrease of the slope of the curve can be misleading in other online image capture applications.

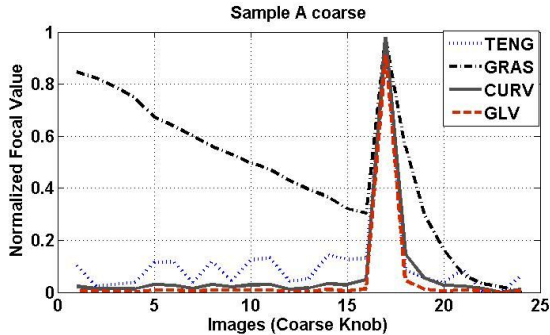


Fig.3. Sample (A) Coarse Knob

5.3. Fine Knob Results

Fig.4 shows a combination of the behavior of the four techniques in calculating the FV of images at different positions predetermined by using the fine knob. 100 images were captured around the area of the most focused image that was determined by the coarse knob in the previous test.

In TENG FV calculation, there are steep fluctuations in FV in early stage images where the FV increases gradually from 0.1 till it reaches its maximum of 1 at image no.60. Furthermore, the FV decreases gradually with sharp fluctuations. For GLV results, the FV is observed to gradually increase starting at 0.575 and increases gradually over a wide range of images ranging from image 1 till it reaches the most focused image that is number 57. Gradual decrease is observed as less focused images are captured and examined. For CURV and GRAS the FV increases smoothly and gradually compared to that of TENG over a wide range of images. For CURV, the maximum FV is 1 at image 60 while in GRAS the maximum FV is 1 at image 59. For both techniques, the FV decreases smoothly over the rest of the images. The observed difference in most focused image FV decision by the four techniques is dependent on the approach each of the different algorithms measures the FV.

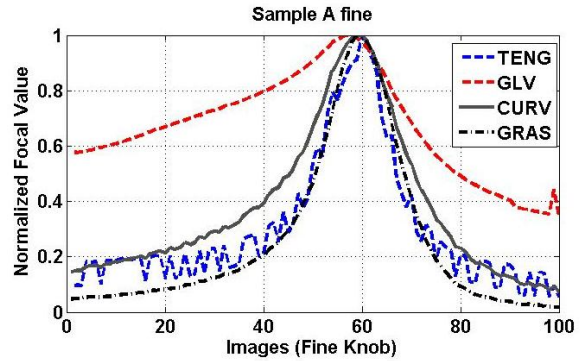


Fig.4. Sample (A) Fine Knob

For more clarification, additional three specimens were tested using the same four algorithms. By using the coarse knob Fig.5, Fig.7 and Fig.9 has successfully identified the same image as the most focused one i.e. image 11 in sample 7, image 22 in sample (40-2) and image 17 in sample 1400. However, in the fine knob curves analysis, all algorithms has successfully identified a range of about 4 images where the most focused image lies , each according to the means of measurement of the algorithm.

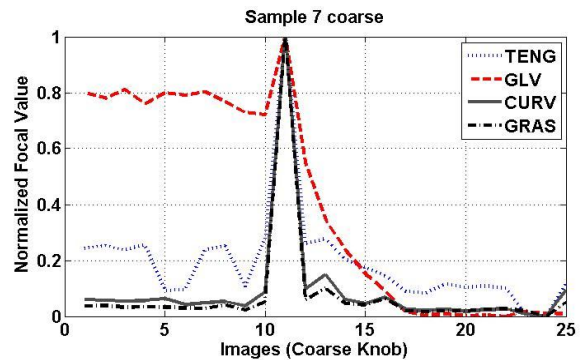


Fig.5. Sample (7) Coarse Knob

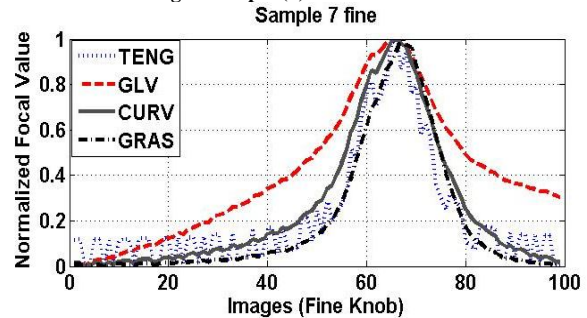


Fig.6. Sample (7) Fine Knob

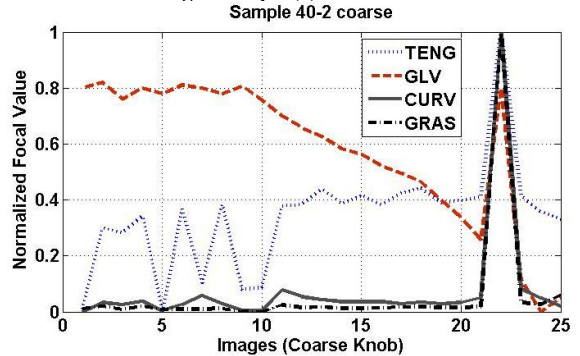


Fig.7. Sample (40-2) Coarse Knob

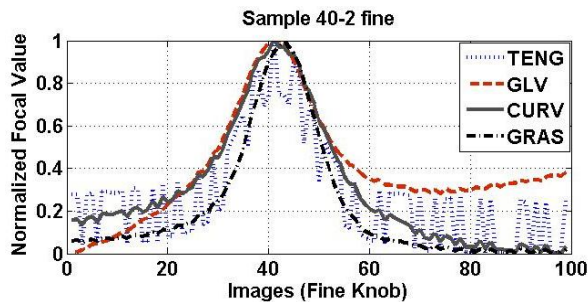


Fig.8. Sample (40-2) Fine Knob

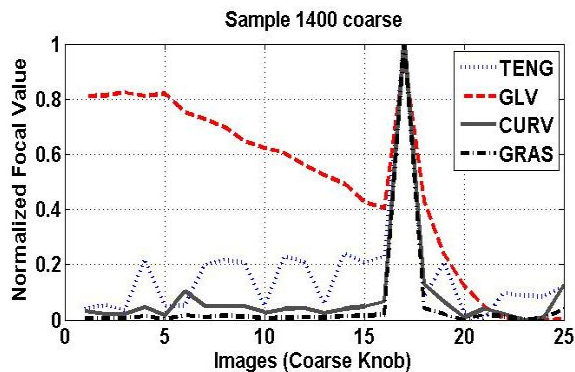


Fig.9. Sample (11) Coarse Knob

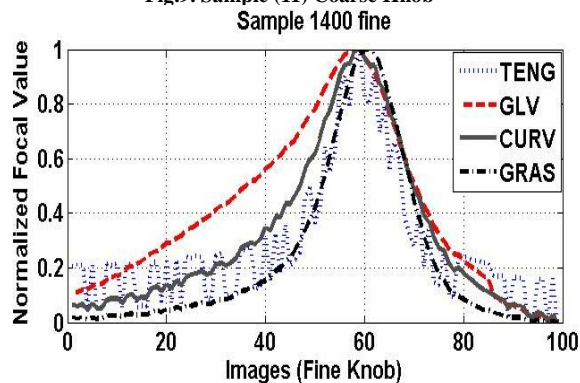


Fig.10. Sample (1400) Fine Knob

In conclusion, the four algorithms have successfully identified the most focused image for all the samples used and analyzed. In both the coarse and fine knob sets of images, GRAS has shown smooth and single peaked curves that identify the most focused image in comparison with the three other tested algorithms. Further image analyses for both coarse and fine image sets can be applied using GRAS later on.

CONCLUSION

This paper discusses an auto focusing system. It is composed of hardware implementation based on a mechanical system and a software based algorithm. The proposed algorithm aims to figure out the most focused image from a series of images of the same scene. This research presents a comprehensive study of four focusing techniques, which are CURV, TENG, GRAS and GLV. A number of microscopic images of different gray cast iron samples were tested under the same conditions using magnification of

(10X). The four techniques have successfully identified the most focused image for all the samples. GRAS demonstrates the best results for both coarse and fine knobs in comparison with the three other tested techniques. This is because the approach FV curve is smooth and the best image has a sharp and clear FV. The proposed focusing system offers significant improvements in accuracy, robustness and speed. It is suitable for implementation in real time processing. Further work will include incorporating image enhancement techniques to improve the final image quality.

REFERENCES

- [1] D. Wang, W. Xing, S. Fan, and W. Wang, "Motorized stereomicroscopy and auto-focusing in computer," in *2012 8th IEEE International Symposium on Instrumentation and Control Technology (ISICT) Proceedings*, 2012, pp. 72–74.
- [2] K. C. Lin, "On Auto Focusing under a Microscopic View," in *IECON 2007 - 33rd Annual Conference of the IEEE Industrial Electronics Society*, 2007, pp. 2938–2943.
- [3] S. Duthaler and B. J. Nelson, "Autofocusing algorithm selection in computer microscopy," in *2005 IEEE/RSJ International Conference on Intelligent Robots and Systems*, 2005, pp. 70–76.
- [4] M. J. Russell, A. Bester, and T. S. Douglas, "Autofocusing a smart microscope for the detection of tuberculosis in sputum smears," in *Proceedings of the 16th Annual Symposium of the Pattern Recognition Association of South Africa (PRASA)*, 2007, pp. 183–189.
- [5] J. M. Geusebroek, F. Cornelissen, a W. Smeulders, and H. Geerts, "Robust autofocusing in microscopy.," *Cytometry*, vol. 39, no. 1, pp. 1–9, Jan. 2000.
- [6] L. Firestone, K. Cook, K. Culp, N. Talsania, and K. Preston, "Comparison of autofocus methods for automated microscopy.," *Cytometry*, vol. 12, no. 3, pp. 195–206, Jan. 1991.
- [7] J. Alvarez-Borrego, "Fast autofocus algorithm for automated microscopes," *Optical Engineering*, vol. 44, no. 6, p. 063601, Jun. 2005.
- [8] A. Santos, C. Ortiz de Solórzano, J. J. Vaquero, J. M. Peña, N. Malpica, and F. del Pozo, "Evaluation of autofocus functions in molecular cytogenetic analysis.," *J. Microsc.*, vol. 188, no. Pt 3, pp. 264–272, 1997.
- [9] F. S. Helmi and S. Scherer, "Adaptive shape from focus with an error estimation in light microscopy," in *ISPA 2001. Proceedings of the 2nd International Symposium on Image and Signal Processing and Analysis. In conjunction with 23rd International Conference on Information Technology Interfaces (IEEE Cat. No.01EX480)*, 2001, pp. 188–193.
- [10] S. Duthaler and B. J. Nelson, "Autofocusing algorithm selection in computer microscopy," in *2005 IEEE/RSJ International Conference on Intelligent Robots and Systems*, 2005, pp. 70–76.
- [11] G. Blahusch, W. Eckstein, and C. Steger, "Calibration of Curvature of Field for Depth from Focus," *International Archives of Photogrammetry Remote Sensing and Spatial Information Sciences*, vol. 34, no. 3/W8, pp. 173–180, 2003.
- [12] G. Cristobal, "Diatom autofocusing in hrightfield microscopy: a comparative study," *IEEE Pattern Recognition*, 2000.
- [13] Vicente, Nathalie B., Javier E. Diaz Zamboni, Javier F. Adur, María F. Izaguirre, and Víctor Casco. "Enhancement of an automatic algorithm for deconvolution and quantification of three-dimensional microscopy images." In *XIV Congreso Argentino de Ciencias de la Computación*. 2008.

- [14] M. Kristan, J. Perš, M. Perše, and S. Kovačič, "A Bayesian-spectral-entropy-based measure of camera focus using a discrete cosine transform," *Pattern Recognition Letters*, vol. 27, no. 13, pp. 1431–1439, 2006.
- [15] B. Goldluecke and D. Cremers, "Introducing total curvature for image processing," in *2011 International Conference on Computer Vision*, 2011, pp. 1267–1274.
- [16] C. Mo and B. Liu, "An auto-focus algorithm based on maximum gradient and threshold," in *2012 5th International Congress on Image and Signal Processing, CISP 2012*, 2012, no. Cisp, pp. 1191–1194.
- [17] S. Pertuz, D. Puig, and M. A. Garcia, "Analysis of focus measure operators for shape-from-focus," *Pattern Recognition*, 2013.
- [18] D. Sen and S. K. Pal, "Gradient histogram: Thresholding in a region of interest for edge detection," *Image Vis. Comput.*, vol. 28, no. 4, pp. 677–695, Apr. 2010.
- [19] X. Tang and P. L. Hostis, "An Auto-Focusing Method in a Microscopic Testbed for Optical Discs," *Journal of Research of the National Institute of Standards and Technology*, vol. 105, no. 4, pp. 565–569, 2000.
- [20] H. Wang, A. Qin, and M. Huang, "Autofocus Method for Digital Holographic Reconstruction of Microscopic Object," *Symposium on Photonics and Optoelectronics*, vol. 2, no. 1, pp. 1–4, Aug. 2009.
- [21] L. I. C. Chiu and C. S. Fuh, "An efficient auto focus method for digital still camera based on focus value curve prediction model," *Journal of Information Science and Engineering*, vol. 26, no. 4, pp. 1261–1272, 2010.
- [22] J. Lorenzo, M. Castrillon, J. Mendez, and O. Deniz, "Exploring the Use of Local Binary Patterns as Focus Measure," *International Conference on Computational Intelligence for Modeling Control & Automation*, 2008.

★ ★ ★